

High-Resolution Magnetometry with a Spinor Bose-Einstein Condensate

M. Vengalattore^{1,*}, J. M. Higbie^{1,*}, S. R. Leslie¹, J. Guzman¹, L. E. Sadler¹, and D. M. Stamper-Kurn^{1,2}

¹*Department of Physics, University of California, Berkeley CA 94720*

²*Materials Sciences Division, Lawrence Berkeley National Laboratory, Berkeley, CA 94720*

(Dated: September 19, 2018)

We demonstrate a precision magnetic microscope based on direct imaging of the Larmor precession of a ⁸⁷Rb spinor Bose-Einstein condensate. This magnetometer attains a field sensitivity of 8.3 pT/Hz^{1/2} over a measurement area of 120 μm², an improvement over the low-frequency field sensitivity of modern SQUID magnetometers. The corresponding atom shot-noise limited sensitivity is estimated to be 0.15 pT/Hz^{1/2} for unity duty cycle measurement. The achieved phase sensitivity is close to the atom shot-noise limit suggesting possibilities of spatially resolved spin-squeezed magnetometry. This magnetometer marks a significant application of degenerate atomic gases to metrology.

Precision magnetometers that map magnetic fields with high spatial resolution have been applied to studies of condensed matter systems [1], biomagnetic imaging [2] and tests of fundamental symmetries [3]. Many of these applications require the measurement of magnetic fields at low (< 10 Hz) frequencies. Current technologies capable of micron-scale magnetic microscopy include superconducting quantum interference devices (SQUIDs), scanning Hall probe microscopes, magnetic force microscopes and magneto-optical imaging techniques [4]. Of these, SQUIDs offer the highest sensitivity, demonstrated at 30 pT/Hz^{1/2} over a measurement area of around 100 μm² [5]. The low-frequency sensitivity of these devices is limited by (1/f) flicker noise of unknown origins [6].

Magnetic fields may also be sensed by detecting the Larmor precession of spin polarized atomic gases. To date, atomic magnetometers have achieved field sensitivities of 0.5 fT/Hz^{1/2} over measurement volumes of 0.3 cm³ [7]. However, attaining high spatial resolution with a hot-vapor medium is precluded by rapid thermal diffusion of the atoms, restricting the minimum resolved length scale of these magnetometers to around 1 mm.

Trapped ultracold gases present an attractive medium for a variety of precision measurements due to their negligible Doppler broadening and long coherence times [8, 9, 10]. Spinor Bose gases, comprised of atoms with non-zero spin, the orientation of which is free to vary, are particularly well suited to magnetic microscopy. In contrast with hot-vapor atomic magnetometers, the suppression of thermal diffusion in a gas through Bose-Einstein condensation enables precise measurements at high spatial resolution. Also, density-dependent mean field shifts, which deleteriously affect other types of precision measurements using dense ultracold gases, do not affect Larmor precession due to the rotational invariance of interparticle interactions in a spinor gas [11, 12].

Here, we perform precise magnetic microscopy with high two-dimensional spatial resolution using a ⁸⁷Rb $F = 1$ spinor Bose-Einstein condensate (BEC). In our magnetometer, longitudinally spin-polarized spinor condensates are prepared in an optical trap. Larmor pre-

cession is induced by tipping the magnetization perpendicular to a bias field imposed along the axis of the condensate. The spins in each region of the condensate then precess at a rate that is proportional to the *local* magnetic field. After a variable integration time, the condensate is probed using magnetization-sensitive imaging to extract the local Larmor phase. The *difference* in this phase between various regions of the condensate reveals the spatial variations of the magnetic field.

The determination of the accrued Larmor phase of a coherent spin state, such as the transversely magnetized condensate, is subject to an uncertainty in the initial phase of $\delta\phi_a = 1/\sqrt{N}$ due to projection noise of measuring N atoms. This noise limits the field sensitivity over a measurement area A to $\delta B = \frac{\hbar}{g\mu_B} \frac{1}{\sqrt{\tau DT}} \frac{1}{\sqrt{\tilde{n}A}}$ where τ is the Zeeman coherence time and \tilde{n} the local column density of the gas. We assume the measurement is repeated over a total measurement time T at a duty cycle D . The $A^{-1/2}$ scaling of field sensitivity with the measurement area A for the atomic magnetometer may be compared with the area scaling for SQUID magnetometers. This scaling ranges between $A^{-3/4}$, for a fixed SQUID sensor coupled optimally to a variable pickup loop, and $A^{-5/8}$, for direct sensing with a SQUID optimized to operate at the quantum limit for the noise energy [13]. For either scaling, the atomic magnetometer outperforms SQUID magnetometers at small measurement areas (Fig. 1).

Optical detection of Larmor precession is limited also by photon shot noise. In this work, the Larmor precession phase is measured by repeated phase-contrast imaging of the condensate using circular polarized light [9]. For our probe detuning of $\delta = 2\pi \times 500$ MHz below the $F = 1 \rightarrow F' = 2$ (D1) transition of ⁸⁷Rb, the phase contrast signal can be written as $s \simeq 1 + 2\tilde{n}\sigma_0(\gamma/2\delta)[c_0 + c_1\langle F_y \rangle]$ where $\sigma_0 = 3\lambda^2/2\pi$ is the resonant cross-section, γ is the natural linewidth and F_y is the projection of the local atomic spin on the imaging axis \hat{y} , which is made perpendicular to the field axis. The detuning-dependent constants $c_0 = 0.118$ and $c_1 = 0.274$ describe the isotropic polarizability and optical activity, respectively. We neglect the effects of linear birefringence ($\propto \langle F_y^2 \rangle$). An es-

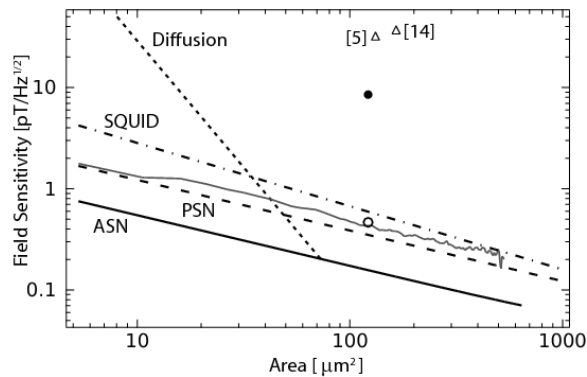


FIG. 1: Field sensitivity for repeated measurements using the spinor BEC magnetometer. Curves marked ASN (PSN) represent atom (photon) shot-noise limited sensitivities, assuming $\tau = 250$ ms, $D = 1$, and the atomic column density and probe light levels for our experiment (see text). Diffusion of magnetization limits the sensitivity for a given length scale by imposing a limit on τ (short dashed line, assuming $D = 1$). The gray line indicates the measured spatial root Allan variance; the sensitivity demonstrated in measurements of an applied localized magnetic field, assuming duty cycles of $D = 0.003$ (●) or $D = 1$ (○), is also shown. Results are compared both to the ideal sensitivity of a quantum-limited SQUID magnetometer (dot-dashed line) and to demonstrated low-frequency sensitivities [5, 14] (Δ).

timate of the Larmor precession phase is obtained by tracking the sinusoidal oscillation of the phase contrast signal across the sequence of phase contrast images. The photon shot-noise limited sensitivity of this estimate is then $\delta\phi_\gamma \approx \sqrt{\frac{2}{\eta N_p} \frac{\sqrt{1+\tilde{n}\sigma_0(\gamma/2\delta)c_0}}{\tilde{n}\sigma_0(\gamma/2\delta)c_1}}$, giving a field sensitivity limit of $\delta B = \frac{\hbar}{g\mu_B} \frac{\delta\phi_\gamma}{\sqrt{\tau DT}}$. Here, η is the detection quantum efficiency and N_p is the total photon fluence, integrated across the multi-pulse imaging sequence, within the region of interest.

For our demonstration, spin-polarized ^{87}Rb condensates of up to 1.4×10^6 atoms were confined in a single-beam optical dipole trap characterized by trap frequencies $(\omega_x, \omega_y, \omega_z) = 2\pi(165, 440, 4.4) \text{ s}^{-1}$ [9]. The tight confinement along the imaging axis (condensate radius $r_y = 2.0 \mu\text{m}$) ensured that the condensate is effectively two-dimensional with respect to spin dynamics. Larmor precession of the condensate was induced in the presence a bias field of 165(7) mG aligned along the long axis of the condensate. A measurement integration time of 250 ms was chosen; at longer times, measurements were hampered by uncontrolled motion of the condensate along the weakly confining dimension (see below).

We operated our ultracold-atom magnetometer under two testing conditions. In one, the magnetometer was used to sense the long length-scale inhomogeneous background magnetic field in our apparatus. While these background fields were partially cancelled by suitable electromagnets, the remaining background typically var-

ied from shot to shot. To account for this fluctuating background, the field profile along the long axis of the condensate was determined by a third-order polynomial fit to the magnetometer measurements [15]. The residuals from this fit were then analyzed to characterize noise limits to our magnetometer.

In the second testing condition, we used the magnetometer to measure a deliberately applied, localized magnetic field. This field was simulated using a circularly polarized laser beam at a wavelength of 790 nm. The choice of wavelength and polarization ensured that this beam imposed a local optically-induced Zeeman shift [16] on the trapped atoms (Fig. 2a). The beam was aligned at an angle $\theta \sim 60^\circ$ to the direction of the bias field, incident and focussed in the plane perpendicular to the imaging axis. The magnetic background for each run of the magnetometer was again determined by third-order polynomial fits, but using measurements from regions far from the localized field. The Zeeman shift due to the localized field was extracted from the residual of this fit.

Measurements of this localized field were affected by small center-of-mass oscillations of the condensate along its long axis. An oscillation with amplitude δz blurs the magnetic landscape and washes out features comparable to or smaller than δz . Unable to eliminate such oscillations completely, we monitored the condensate motion for each run of the magnetometer by a sequence of four images spaced at a quarter period of the axial trap frequency, taken prior to the Larmor imaging sequence. We discarded measurements for which an excursion comparable to the width of the localized field was indicated.

Two-dimensional maps of the magnetic field were obtained from a pixel-by-pixel analysis of the Larmor precession phase at each coordinate within the profile of the condensate (Fig. 2b). The frame-to-frame variation of this signal showed the characteristic oscillations due to Larmor precession as well as an overall decay of the condensate number due to off-resonant scattering of probe light. This decay was taken into account in obtaining an unbiased estimate of the local Larmor phase. Our 2D approach was found to be susceptible to imaging aberrations, primarily in the narrow (\hat{x}) dimension of the gas.

Alternately, more robust measurements were obtained by integrating the field measurement over the \hat{x} direction to reduce measurements to a single resolved direction along the long axis (\hat{z}) of the gas. For this, the aberrated signal profile in the \hat{x} direction was determined at each z coordinate in the images from averages over the multiple frames. The phase-contrast signal height in each image frame and at each z coordinate was then determined. 1D phase profiles were obtained as before (Fig. 2c).

The demonstrated sensitivity of our magnetometer is shown in Fig. 1. The spatial root Allan variance from the 1D data was determined for each of 15 runs of the magnetometer under the first testing conditions (magnetic background only) and then averaged. Here, the

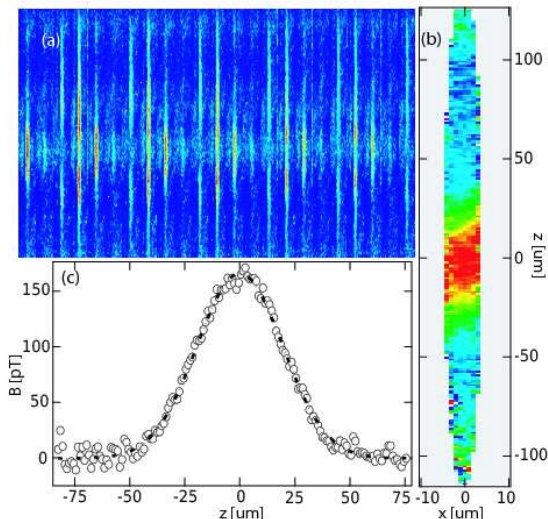


FIG. 2: (a) Sequence of phase contrast images of a condensate under the influence of a local optically-induced Zeeman shift. (b) The resulting 2-D map of the magnetic field obtained by a pixel-by-pixel estimation of the Larmor precession phase. (c) 1-D phase profile showing the applied field inhomogeneity. The peak strength of the field as determined by this single-shot measurement is 166.2 ± 1.2 pT.

measurement *area* is determined by accounting for the effective $5.3 \mu\text{m}$ length over which the aberrated signals are averaged in the \hat{x} direction. This noise level matches closely with photon shot-noise estimates and is ~ 3 times that due to atomic shot-noise given the number of atoms in the corresponding areas. Excess noise for areas larger than about $20 \mu\text{m}^2$ was found to correlate with the local intensity of the probe light, an effect we attribute to probe-light induced shifts of the Larmor precession frequency during imaging. This noise can be reduced by using a linearly polarized probe with a more homogenous intensity profile and by carefully aligning the magnetic bias field to be perpendicular to the imaging axis.

Results from measurements under the second testing condition (background plus localized field) are shown in Fig. 3. Here, the strength of the applied field (peak value of Gaussian fits) was measured repeatedly at several powers of the field-inducing laser beam. From all these measurements, a calibration between the laser power and the localized field strength was obtained. From the residual scatter in the measurements, we determine the (rms) sensitivity of our Larmor precession phase measurements as 1.0×10^{-2} rad, corresponding to a single-shot field sensitivity of 0.9 pT over the $120 \mu\text{m}^2$ area under the Gaussian field profile. This sensitivity was demonstrated for field strengths up to 60 pT. A marginally larger variance for higher fields points to the existence of small systematic effects, e.g. residual motion of the condensate or variations in the localized field strength. Averaging over the entire range of measurements shown in Fig. 3 yields a

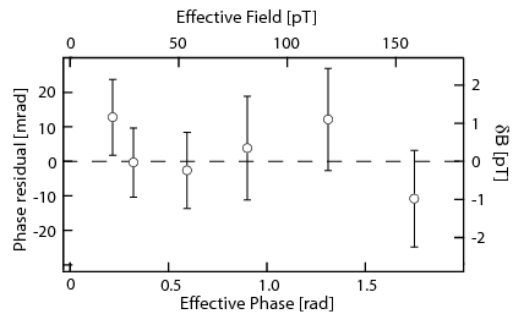


FIG. 3: Single-shot measurements of the localized magnetic field imposed by a laser beam focused to $\sigma = 24 \mu\text{m}$ rms width. Residuals from a linear fit, calibrating the field magnitude *vs* laser power, are shown. Error bars indicate standard deviations for 10 measurements per setting. The measurement time was 250 ms.

phase sensitivity of 1.2×10^{-2} rad.

Under repeated operation, our magnetometer, with a low duty cycle of just $D = 3 \times 10^{-3}$, attains a field sensitivity of $8.3 \text{ pT}/\text{Hz}^{1/2}$, an improvement over that demonstrated for low-frequency (< 10 Hz) field measurements with modern SQUID magnetometers [5, 14]. Plausible extensions of current cold-atom experimental methods should enable duty cycles of order unity. At full duty cycle, our demonstrated single-shot sensitivity would correspond to a field sensitivity of $0.5 \text{ pT}/\text{Hz}^{1/2}$.

As discussed above, in the photon shot-noise limit, the sensitivity of an atomic magnetometer increases with increasing probe fluence. While calculations based on linear Raman scattering rates indicated that reliable phase measurements could be obtained even at a fluence of 3400 photons/ μm^2 per frame, it was found that the light induced losses of the condensate far exceeded those predicted by the calculations. The discrepancy was attributed to superradiant Raman scattering of atoms into the $F = 2$ hyperfine states, in which atoms would no longer be observed by our probe. To counter this problem, the superradiant gain was reduced by lowering the probe intensity. Each frame in the imaging sequence was obtained by integrating the light from four pulses of light, each of duration $2.2 \mu\text{s}$ and spaced by the Larmor period of $\sim 10 \mu\text{s}$. We also increased the motional decoherence of the $F = 2$ atoms produced during superradiance by their preferential scattering of incident light resonant with the $F = 2 \rightarrow F' = 3$ (D2) transition. Together, these strategies enabled a probe fluence of 750 photons/ μm^2 per frame.

Our magnetometry medium, though Bose condensed, is still a gas in which atoms are free to move. Thus, in determining the phase shift accrued due to a local magnetic field, one must consider atomic motion due to both quantum-mechanical and classical effects. For instance, imposing a weak inhomogeneous field of characteristic length σ leads to quantum diffusive motion of the fluid.

For times $\tau > \tau_Q = m\sigma^2/\hbar$, with m the atomic mass, the motion of the spinor gas will greatly reduce the phase accrued due to Larmor precession. This evolution can be considered to be the quantum limit of thermal diffusion observed in NMR studies [17]. In our experiment, the condition $\tau = 250 \text{ ms} > \tau_Q$ is reached at length scales below $10 \text{ } \mu\text{m}$ (Fig. 1). For integration times $\tau \ll \tau_Q$, effects of quantum diffusion require that phase measurements ϕ be corrected by an amount $\delta\phi/\phi \sim (\tau/\tau_Q)^4$.

An inhomogeneous magnetic field also exerts forces on magnetic dipoles. In the extreme case of static inhomogeneous fields with a Zeeman energy comparable to the chemical potential ($\sim 10^5$ times larger than those studied in this work), these classical forces can modify the density distribution of the condensate [18]. In our case, these forces result in small corrections and limits to the accrued Larmor phase. The field strength B and a characteristic length σ for its variation define a classical time scale $\tau_C = \sqrt{m\sigma^2/\mu_B B}$, the time taken by an atom to move σ when accelerated by this field. For an integration time τ , this classical motion imposes a limit on the maximum detectable phase shift (when $\tau = \tau_C$) of $\phi_m \simeq \tau_Q/\tau$. It should be noted that neither the diffusion of an imprinted phase nor the limitation on the dynamic range are fundamental; both can be eliminated by constraining atomic motion, e.g. by imposing an optical lattice potential.

To observe the dilution of magnetization due to atomic motion, we imposed a light-induced magnetic field localized to a beam waist of $5.4 \text{ } \mu\text{m}$ onto the transversely-magnetized spinor condensate. Following a 5 ms exposure to the field-inducing laser beam, the condensate magnetization was allowed to evolve freely for variable time before being probed. During this evolution, the imprinted Larmor phase diminished in peak height and grew in extent, matching well with calculations based on a non-interacting spinor gas in a localized field (Fig. 4).

In conclusion, we have demonstrated a spinor-BEC magnetometer, a powerful application of ultracold atoms to precision measurement of scientific and technological significance. Inasmuch as the Larmor precession phase represents the phase relations among BECs in several Zeeman states, this magnetometer can be regarded as a condensate interferometer with high temporal and spatial resolution. The single-shot phase sensitivity and shot-to-shot variations of 10 mrad achieved here represent an order of magnitude improvement over the performance of current BEC interferometers.

The demonstrated phase sensitivity is close to the atom shot-noise limit. This augurs spin-squeezed magnetometry via continuous quantum non-demolition measurements of the condensate [19] and novel spatially and temporally resolved studies of spin squeezed ensembles. Finally, the high spatial resolution and sensitivity of the spinor magnetometer render it a powerful detector of quantum spins in optical lattices and may facilitate time-

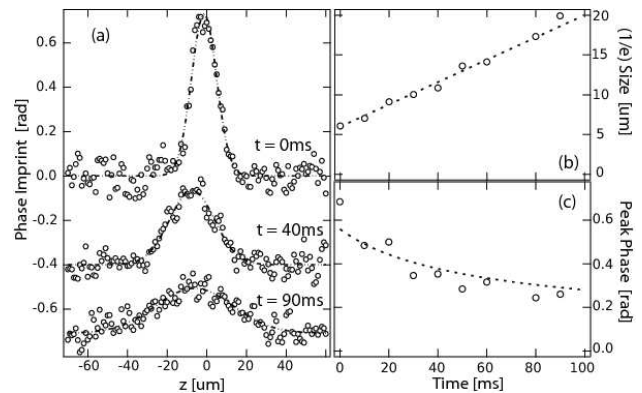


FIG. 4: Quantum evolution of an imprinted phase. (a) Cross sections of the phase imprint after a free evolution time $t = 0, 40$ and 90 ms. Traces are offset for clarity. (b) The $1/e$ width of the imprinted phase. The dashed line corresponds to numerical simulations based on a non-interacting spinor gas. (c) The peak phase *vs* the free evolution time. The dashed line corresponds to the expected scaling imposed by normalization of magnetization.

resolved, nondestructive studies of frustration, dipolar interactions and disorder in such systems.

We thank D. Budker and J. Clarke for helpful discussions. This work was supported by the NSF and the David and Lucile Packard Foundation. S. R. L. acknowledges support from the NSERC.

* These authors contributed equally to this work.

- [1] C. C. Tsuei and J. R. Kirtley, *Rev. Mod. Phys.* **72**, 969 (2000).
- [2] K. Kobayashi and Y. Uchikawa, *IEEE Trans. Mag.* **39**, 3378 (2003).
- [3] L. R. Hunter, *Science* **252**, 73 (1991).
- [4] S. J. Bending, *Adv. Phys.* **48**, 449 (1999).
- [5] J. R. Kirtley *et al*, *Appl. Phys. Lett.* **66**, 1138 (1995).
- [6] R. H. Koch *et al*, *J. Low Temp. Phys.* **51**, 207 (1983).
- [7] I. K. Kominis *et al*, *Nature* **422**, 596 (2003).
- [8] P. Treutlein *et al*, *Phys. Rev. Lett.* **92**, 203005 (2004).
- [9] J. M. Higbie *et al*, *Phys. Rev. Lett.* **95**, 050401 (2005).
- [10] G. B. Jo *et al*, *cond-mat/0608585* (2006).
- [11] T. L. Ho, *Phys. Rev. Lett.* **81**, 742 (1998).
- [12] T. Ohmi and K. Machida, *J. Phys. Soc. Jpn.* **67**, 1822 (1998).
- [13] R. H. Koch, D. J. Van Harlingen and J. Clarke, *Appl. Phys. Lett.* **38**, 380 (1981).
- [14] T. S. Lee, E. Dantsker and J. Clarke, *Rev. Sci. Instr.* **67**, 4208 (1996).
- [15] Based on the geometry of the apparatus and the location of magnetic field sources, we estimate field variations across the condensate due to fourth order and higher terms to be $\ll 1$ fT, negligible even at the high precision of the spinor magnetometer.
- [16] J. Dalibard and C. Cohen-Tannoudji, *J. Opt. Soc. Am. B* **6**, 2023 (1989).
- [17] H. Carr and E. Purcell, *Phys. Rev.* **94**, 630 (1954).

- [18] S. Wildermuth *et al*, Nature **435**, 440 (2005).
- [19] A. Kuzmich *et al*, Europhys. Lett. **42**, 481 (1998).